Taylor & Francis
Taylor & Francis Group

The role of mitochondrial alterations in the combined toxic effects of human immunodeficiency virus Tat protein and methamphetamine on calbindin positive-neurons

Dianne Langford,[1] Aline Grigorian,[1] Rosemary Hurford,[2] Anthony Adame,[2] Leslie Crews,[2] and Eliezer Masliah[1,2]

Departments of [1]Pathology and [2]Neurosciences, University of California, San Diego, La Jolla, California, USA

The use of methamphetamine (METH) continues to increase the risk of human immunodeficiency virus (HIV) transmission within both homosexual and heterosexual drug abuser groups. Neurological studies indicate that the progression of HIV encephalitis is also enhanced by illicit drug use. Recently, the authors' studies in the postmortem brains of HIV-positive METH users have shown that the combined effects of HIV and METH selectively damage calbindin (CB)-immunoreactive nonpyramidal neurons, which may contribute to the behavioral alterations observed in these patients. To better understand the mechanisms of toxicity associated with exposure to HIV and METH, neuronal survival, phenotypic markers, levels of oxidative stress, and mitochondrial potential were assessed *in vitro* in the hippocampal neuronal cell line, HT22, and in primary human neurons exposed to the HIV Tat protein and/or METH. Both Tat and METH were toxic to neurons in a time- and dose-dependent fashion. Neurons exposed to a combination of Tat and METH displayed early evidence of neuronal damage at 6 h, characterized by a decrease in CB and microtubule-associated protein 2 (MAP2) immunoreactivity followed by more extensive cell death at 24 h. Loss of CB immunoreactivity associated with the combined exposure to Tat and METH was accompanied by mitochondrial damage with increased levels of oxidative stress. The toxic effects of Tat and METH were inhibited by blocking mitochondrial uptake of intracellular calcium, whereas blocking calcium flux in the endoplasmic reticulum or from the extracellular environment had no effect on Tat and METH toxicity. These studies indicate that *in vitro*, when combined, the HIV protein Tat and METH damage CB-immunoreactive nonpyramidal neurons by dysregulating the mitochondrial calcium potential. In combination, Tat and METH may increase cell injury and death, thereby enhancing brain metabolic disturbances observed in HIV-positive METH users in clinical populations. *Journal of NeuroVirology* (2004) 10, 327–337.

Keywords: calbindin; HIVE; methamphetamine; neurodegeneration; Tat

Introduction

Methamphetamine (METH) use is often associated with behaviors that increase the risk for the transmission of human immunodeficiency virus (HIV). HIV-negative men who have sex with men and use METH are 2.9 times more likely to become infected with HIV than non-METH users of the same group (Chesney *et al*, 1998). HIV infection is more frequent in METH-using heterosexuals than in non-users as well (Molitor *et al*, 1999). Furthermore, the onset of HIV encephalitis (HIVE) in drug abusers is both more rapid and more severe (Bell *et al*, 1998; Bouwman *et al*, 1998; Nath *et al*, 2001). Studies in the postmortem brains of HIV-positive patients with and without a history of METH use revealed that HIVE patients who used METH had a higher frequency

of ischemic events and a more severe microglial reaction, but a significantly lower brain viral burden, and less severe forms of encephalitis, than HIVE patients who were non-METH users (Langford *et al*, 2003). Furthermore, in METH-using HIVE patients, extensive loss of calbindin (CB)-immunoreactive interneurons accompanied by aberrant sprouting, with no evidence of ischemic injury, was observed. These studies indicate that the combined effects of METH and HIV can selectively damage CB-immunoreactive nonpyramidal neurons. However, the mechanisms responsible for neuronal damage resulting from the synergistic effects of HIV and METH abuse are not clearly understood.

Nath *et al* suggest that acceleration in the cognitive impairments of some HIV patients who use drugs may be due to destabilization of neuronal functioning by these drugs of abuse, and when combined with HIV toxicity, may result in synergistic neurotoxicity (Nath *et al*, 2002). Tat and METH have been shown, both independently and in combination, to promote oxidative stress by alterations in excitotoxic neurotransmitter release (Aksenov *et al*, 2001; Berman and Hastings, 1999; Bonavia *et al*, 2001; Cadet and Brannock, 1998; Eisch *et al*, 1996; Imam and Ali, 2000; Love, 1999; Ohmori *et al*, 1996; Stephans and Yamamoto, 1994). Also, Flora *et al* have shown that HIV Tat protein and METH act synergistically to stimulate the activation of transcription factors, such as nuclear factor κB (NFκB), activator protein-1 (AP-1), and c-AMP–regulated extracellular binding protein (CREB), which induce the expression of genes, including tumor necrosis factor-α (TNF-α), interleukin-1β (IL-1β), and intercellular adhesion molecule-1 (ICAM-1), involved in redox-regulated inflammatory pathways in the brain (Flora *et al*, 2003). Alterations in neurotransmitter release and excitotoxicity can cause mitochondrial destabilization and depolarization leading to decreased cell fitness. During excitotoxic conditions, disruptions in the intracellular calcium-buffering capacity can cause accumulation of mitochondrial calcium, leading to neuronal dysfunction (Kruman *et al*, 1998; Stout *et al*, 1998). Studies by Turchan *et al* using dopaminergic neurons in a human brain cell culture model show that in combination, Tat and METH significantly decrease mitochondrial membrane potential (Turchan *et al*, 2001). Thus, in combination, METH and Tat may increase cell injury and death, thereby enhancing brain metabolic disturbances observed in HIV-positive METH abusers in clinical populations.

Taken together, these studies suggest that Tat and METH may contribute to disruptions in the calcium-buffering capacity of the neuron. Along with this possibility, these alterations may be also related to the cellular loss of calcium-binding proteins such as CB. Therefore, to further characterize potential mechanisms responsible for neuronal damage observed in the brains of HIV-positive METH using patients, we assessed *in vitro* cell survival, neuronal phenotypic

markers, levels of oxidative stress, and mitochondrial potential in neurons exposed to Tat and/or METH. These studies indicate that *in vitro,* the combined effects of the HIV protein Tat and METH damage CB-immunoreactive nonpyramidal neurons by dysregulating the mitochondrial calcium potential.

Results

Immunocytochemical characterization of HT22 and human neuronal (HN) cells
To begin exploring possible mechanisms of METH and Tat toxicity on CB-immunoreactive neuronal populations, *in vitro* studies were performed using mouse hippocampal HT22 cells and primary human neuronal (HN) cells. Further characterization by immunocytochemistry and laser scanning confocal microscopy (LSCM) showed that HT22 and HN cells display robust CB (Figure 1A, F), microtubule-associated protein 2 (MAP2) (Figure 1B, G), and γ-amniobutyric acid (GABA) (Figure 1C, H) immunoreactivity and moderate glutamate (Figure 1D, I) immunoreactivity. No reactivity was observed with antibodies against parvalbumin (PV) (Figure 1E, J), *N*-methyl D-aspartate (NMDA; data not shown) or astrocyte-specific glial fibrillary acidic protein (GFAP; data not shown). These data suggest that HT22 and HN cells are similar in profile to the CB positive neuronal population vulnerable to METH and HIV in patients (Langford *et al*, 2003).

Tat and METH are toxic to neurons in a dose- and time-dependent manner
To determine the effects of Tat and/or METH on HT22 and HN cells, viability assays were conducted on neurons exposed to Tat or METH alone, or in combination at different concentrations and for varying lengths of time. Cell death was determined by trypan blue exclusion, TdT-mediated dUTP nick-end labeling (TUNEL) and fluorescein diacetate (FA)/propidium iodide (PI) viability assays. HT22 cells treated with varying concentrations of either Tat (0, 5, 25, 50, 100, and 250 nM) or METH (0, 5, 25, 50, 100, and 250 μM) for 24 h showed a nearly linear increase in cell death with increased doses of either Tat or METH (Figure 2A). Exposure to a 250-nM Tat dose or a 250-μM METH dose resulted in the maximal observed cell death at 35.5% and 68%, respectively (Figure 2A). Twenty-four-hour exposures of HT22 cells to 50 nM Tat or 50 μM METH resulted in 24.4% and 23.6% cell death, respectively. Furthermore, doses of 50 nM Tat and 50 μM METH were not significantly different from one another ($P = .667$), but were significantly greater than cell death observed in untreated cells ($P < .0001$ and $P < .0001$, respectively). Time course studies (Figure 2B) with 50 nM Tat or 50 μM METH showed increased cell death over time at each time point compared to untreated cells. Increases in cell death were significant for cells treated with either
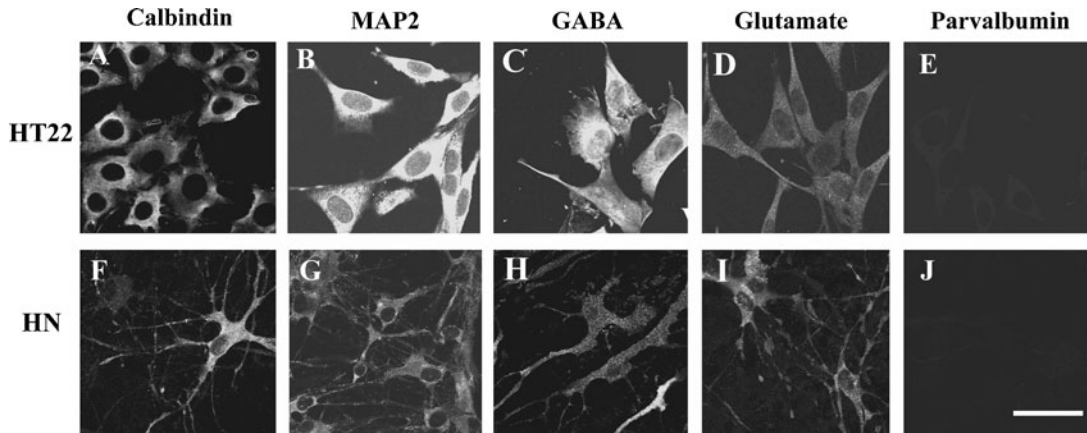
Tat and methamphetamine in neuronal toxicity
D Langford *et al*
329

Figure 1 Characterization of immunoreactivity patterns for neural markers in HT22 and HN cells. All images were imaged with the laser scanning confocal microscope. Panels **A** to **E** are HT22 cells; panels **F** to **J** are HN cells. Intense immunoreactivity was observed with antibodies against the calcium binding protein, calbindin (**A** and **F**), the microtubule-associated protein (MAP2) (**B** and **G**), and the inhibitory neurotransmitter, γ-aminobutyric acid (GABA) (**C** and **H**). Moderate immunoreactivity was observed with an antibody against the excitotory neurotransmitter, glutamate (**D** and **I**). No immunoreactivity with an antibody against the parvalbumin was observed (**E** and **J**). Bar = 25 microns.

Tat or METH at 24 h ($P = .0258$ and $P = .0087$, respectively) and 48 h ($P = .0438$ and $P = .0391$, respectively). No significant cell death was observed with Tat, METH, or Tat plus METH at 6 h (Figure 2B). In contrast, compared to both the Tat and METH treatments alone, the combined Tat/METH exposure resulted in significantly greater cell death at 24 h ($P < .0001$ and $P < .0001$, respectively). Phase-contrast images of HT22 cells treated with Tat and METH for 24 h confirmed previous results showing that a combination of Tat and METH results in increased neuronal cell death compared to singly treated or untreated cells (Figure 2C–F). Consistent with these observations, trypan blue exclusion assays

confirmed that while Tat or METH (50 nM, 50 μM, respectively) treatment alone for 24 h resulted in approximately 20% cell death, the combination of the two resulted in 40% cell death (Figure 2B).

Similarly, HN cells exposed to varying concentrations of either Tat (0, 50, 150, 250, and 500 nM) or METH (0, 50, 150, 250, and 500 μM) for 24 h showed increasing cell death correlating with increased doses of either Tat or METH (data not shown); however, HN cells were more resistant to Tat and METH toxicity than the HT22 cells. Thus, for time course experiments, HN cells were treated with Tat at 250 nM and METH at 100 μM. At these concentrations the combination of Tat and METH did not result in significant
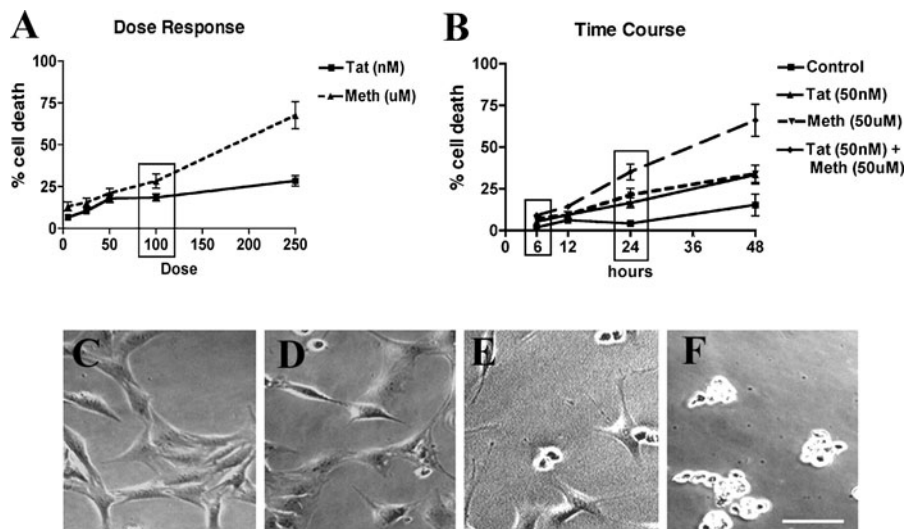

Figure 2 Viability of HT22 cells exposed to Tat and/or METH. Cell viability was assessed by the trypan blue dye exclusion assay. (**A**) Dose response of HT22 cells to increasing doses of Tat (0 to 250 nM) or methamphetamine (METH) (0 to 250 μM) for 24 h. (**B**) Time course of HT22 cells exposed to Tat (50 nM) or METH (50 μM) from 0 to 48 h. *$P < .05$ by one-factor ANOVA with Fisher's post hoc test. Percent cell death is represented by the combination of results from four separate experiments. Phase-contrast images of HT22 cells untreated (**C**), treated with 50 nM Tat (**D**), 50 μM METH (**E**), or a combination of both (50 nM Tat and 50 μM METH) (**F**). Bar = 25 microns.

neuronal cell death at 6 h, whereas at 24 h, these doses promoted an average of 28% cell death (not shown). Taken together, viability studies suggest that both Tat and METH are toxic to HT22 and HN cells in a time- and dose-dependent manner and that in combination, exposure to Tat and METH results in significantly increased cell death at 24 h.

Decreased calbindin expression in neurons treated with Tat and METH
Immunocytochemical analyses and LSCM were used to determine the effects of Tat and METH on the levels and patterns of CB and MAP2 immunoreactivity in treated neurons. Both HT22 and HN cells displayed strong CB and MAP2 immunoreactivity that was diffusely distributed in the cytoplasm (Figure 1A, B, F, G). Compared to controls, after treatment with Tat or METH alone for 6 h, no significant decrease in levels of CB immunoreactivity was detected (Figure 3E). In contrast and compared to controls (Figure 3A, F), levels of CB immunoreactivity decreased by 34.6% after 24 h treatment with 50 nM Tat (Figure 3B, F) and by 40% with 50 μM METH (Figure 3C, F) in HT22 cells. After 48 h of treatment or when concentrations of greater than 50 nM Tat or 50 μM METH were used, CB immunoreactivity in HT22 cells decreased over 90% (data not shown). Furthermore, after Tat and/or METH treatment for 24 h, CB immunoreactivity was redistributed from throughout the cytoplasm to the periphery of the cells (compare Figure 3A with B to D).

Further studies showed that compared to controls (Figure 3G, L), levels of neuronal MAP2 immunoreactivity decreased 10% to 23% after 24 h treatment with either 50 nM Tat (Figure 3H, L) or 50 μM METH (Figure 3I, L). After 48 h of treatment or at doses greater

than 100 nM Tat or 100 μM METH, levels of MAP2 immunoreactivity in HT22 cells decreased over 90% (data not shown). MAP2 cellular distribution was not affected by Tat and/or METH treatments (compare Figure 3G with H to J). Although exposure of HT22 cells to Tat or METH alone for 6 h did not significantly decrease levels of CB and MAP2 immunoreactivity, the combination of Tat and METH for the same length of time resulted in a significant decrease in the levels of CB (Figure 3E) and MAP2 (Figure 3K) immunoreactivity. Similarly, although exposure to either Tat or METH alone for 24 h moderately decreased the levels of CB and MAP2 immunoreactivity, the combination of these neurotoxins for 24 h (Figure 3D, J) resulted in a significantly greater decrease in levels of CB immunolabeling (78.4%, $P < .0001$; Figure 3F) and MAP2 (85.9%, $P < .0001$; Figure 3L). Consistent with these results in HT22 cells, exposure of HN cells to Tat (250 nM) and METH (100 μM) resulted in decreased CB and MAP2 immunoreactivity at 24 h (data not shown). In conclusion, immunocytochemical studies suggest that Tat and METH cooperate to promote a more profound decrease in CB and MAP2 immunoreactivity in neurons compared to neurons treated with either Tat or METH alone.

Tat and METH toxicity is blocked by inhibiting mitochondrial calcium flux
Because alterations in CB immunoreactivity were associated with the neuronal damage triggered by the combination of Tat and METH, it is possible that the neurotoxic effects of dysregulation in calcium homeostasis might play a role in the mechanisms of neurodegeneration. To investigate this possibility, neurons were treated with calcium flux blockers before challenge with Tat and METH. Blocking
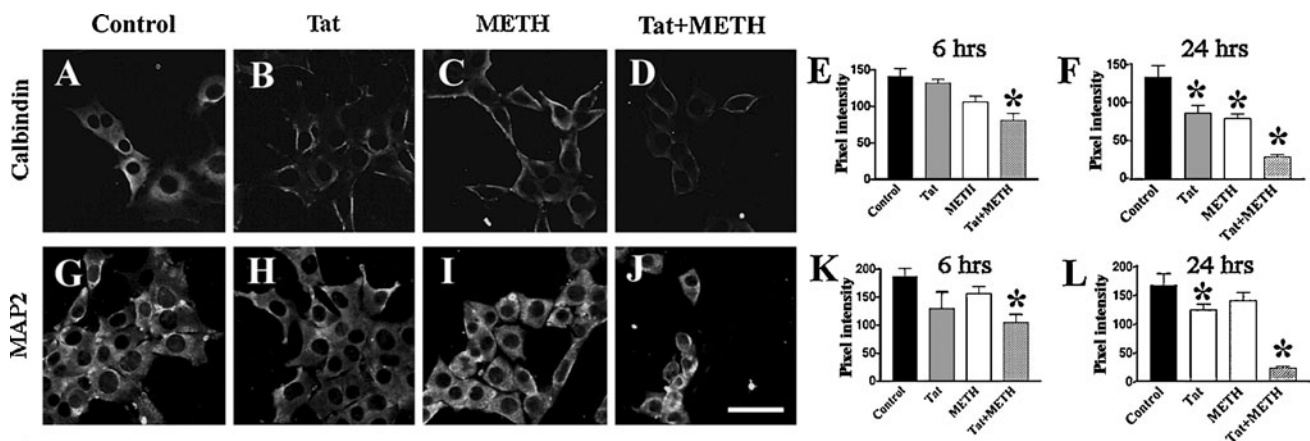

Figure 3 Comparison of the effects of Tat and/or METH treatment on HT22 cells. Cells in panels **A** and **G** are untreated controls. Cells in panels **B** and **H** were exposed to Tat (50 nM, 24 h). Cells in panels **C** and **I** were exposed to METH (50 μM, 24 h). Cells in panels **D** and **J** were exposed to both Tat (50 nM) and METH (50 μM) for 24 h. Panels **E**, **F**, **K**, and **L** show quantitative analyses for each experiment. Cells in panels **A** to **D** were immunolabeled with an antibody against CB and cells in panels **G** to **J** were immunolabeled with an antibody against MAP2 and imaged with a LSCM. (**E**, **F**) HT22 cells treated with Tat and METH for 6 h (**E**) or 24 h (**F**) showed significant decreases in CB immunoreactivity. $^*P < .05$ by one-factor ANOVA with Fisher's post hoc test when compared to the untreated control. (**K**, **L**) HT22 cells treated with Tat and METH for 6 h (**K**) or 24 h (**L**) showed significant decreases in MAP2 immunoreactivity. $^*P < .05$ by one-factor ANOVA with Fisher's post hoc test when compared to the untreated control, Tat, or METH. Bar = 25 microns.
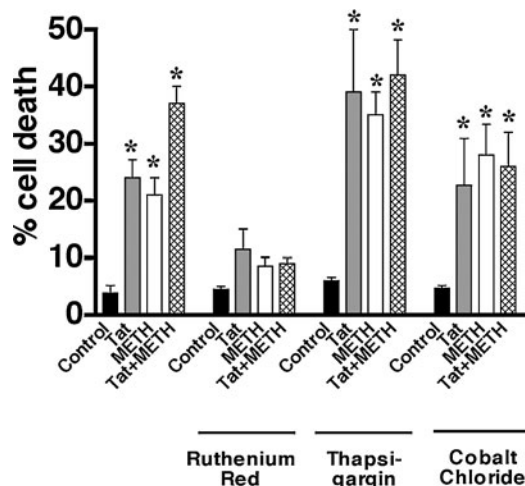
Figure 4 Comparison of the effects of Tat and/or METH treatment on HT22 cell survival in the presence of calcium inhibitors. Cells were treated with either Tat or METH or with a combination of both after a 30-min exposure to ruthenium red to block mitochondrial flux, thapsigargin to block endoplasmic reticulum calcium flux, or cobalt chloride to prevent extracellular calcium influx. Cell viability was assessed by the trypan blue exclusion assay. $^*P < .05$ by one-factor ANOVA with Fisher's post hoc test when compared to the untreated control, Tat, METH, or Tat and METH.

mitochondrial calcium flux with ruthenium red (RR) prior to Tat, METH, and Tat/METH exposure decreased cell death significantly, compared to cells exposed to Tat, METH and Tat/METH without RR ($P = .011$, $P = .0013$, $P < .0001$, respectively, Figure 4). Conversely, neither thapsigargin (TH), an endoplasmic reticulum calcium flux blocker, nor cobalt chloride (CC), an extracellular calcium flux blocker, significantly affected cell death in either HT22 or HN cells treated with Tat, METH, or Tat/METH (Figure 4). RR, TH, or CC treatment alone did not significantly affect cell viability (Figure 4). These results suggest that mitochondrial calcium homeostasis rather than endoplasmic reticulum or extracellular calcium flux is involved in Tat/METH neuronal disruptions.

Tat and METH disrupt the mitochondrial calcium buffering capacity
To further investigate the mitochondrial role in Tat/METH-mediated neuronal injury and death, dyes specific for mitochondria were used to examine mitochondrial mass and membrane potential of HT22 and HN cells treated with Tat and/or METH. MitoTracker dyes are fluorescent mitochondrial markers that bind free sulfhydryls and have been successfully used in neurons (Buckman *et al*, 2001). MitoTracker Green is insensitive to mitochondrial membrane potential and is used to assess mitochondrial shape and mass (Poot *et al*, 1996), whereas MitoTracker Red is rapidly taken up into negatively charged mitochondria, and has been shown to indicate membrane potential and oxidative damage in neurons (Buckman *et al*, 2001).

As evidenced by MitoTracker Red staining, compared to untreated cells (Figure 5A, J), significant in-

creases in oxidative stress were observed in HT22 neurons exposed to Tat (79.9% above control, $P = .0008$, Figure 5B, J) or METH (85.4% above control, $P < .0001$; Figure 5C, J). An even more dramatic increase in oxidative stress was observed in HT22 cells treated with both Tat and METH (91.6% above control, $P < .0001$; Figure 5D, J). Likewise, in combination, Tat/METH exposure increased oxidative stress above single Tat and METH treatments by 58.2% and 42.6%, respectively (Figure 5J). The mitochondrial mass within cells, as determined by MitoTracker Green staining, appeared equivalent between untreated and Tat and/or METH treated neurons with no significant differences observed (Figure 5I). To further confirm whether the combined effects of Tat and METH on mitochondrial functioning resulted in increased oxidative stress, HT22 cells were labeled with 2′,7′-dichlorodihydrofluorescein diacetate (H_2DCFDA) and imaged with the LSCM. These studies showed that at 6 h, Tat, METH, and Tat plus METH increased H_2DCFDA reactivity significantly above controls (Figure 6A to E). However, in combination for 6 h, Tat and METH toxicity was not significantly different from Tat or METH treatment alone. On the other hand, after 24 h, Tat and METH combined increased H_2DCFDA reactivity significantly more than either Tat or METH alone and above controls (Figure 6F to J).

To investigate the effect of blocking mitochondrial calcium flux on Tat-METH–induced cellular oxidative stress, HT22 cells were exposed to RR prior to Tat and/or METH treatment and then stained with MitoTracker dyes, as described above. In the presence of RR alone, no differences were observed in mitochondrial mass among controls, cells treated with Tat and/or METH, or in cultures with no RR (Figure 5A to I). HT22 cells pretreated with RR prior to 50 nM Tat showed a 30% decrease in oxidative stress compared to Tat-treated neurons without RR (Figure 5B, F, J). Similarly, HT22 cells pretreated with RR prior to 50 μM METH showed a significant decrease (54.7%, $P = .0010$) in oxidative stress compared to neurons treated with METH alone (Figure 5C, G, J). HT22 cells pretreated with RR followed by a combination of both Tat and METH showed a dramatic decrease in oxidative stress (63%, $P < .0001$) compared to Tat/METH treated neurons without RR (Figure 5D, H, I).

Likewise, studies of mitochondrial mass and oxidative state in HN cells exposed to Tat and/or METH confirmed that in combination, Tat and METH significantly increased oxidative stress above levels observed in HN cells treated with Tat (26.2%, $P = .0004$; Figure 7A, B, J) or METH alone (42.9%, $P < .0001$; Figure 7A, C, J). However, blocking mitochondrial calcium flux with RR (Figure 7E–H, J) prevented Tat-METH–induced increases in radical oxygen species as determined by MitoTracker Redox Red staining (Figure 7J). Pretreatment of HN cells with RR significantly decreased both Tat and METH induced oxidative stress by 56.0% ($P < .0001$) and
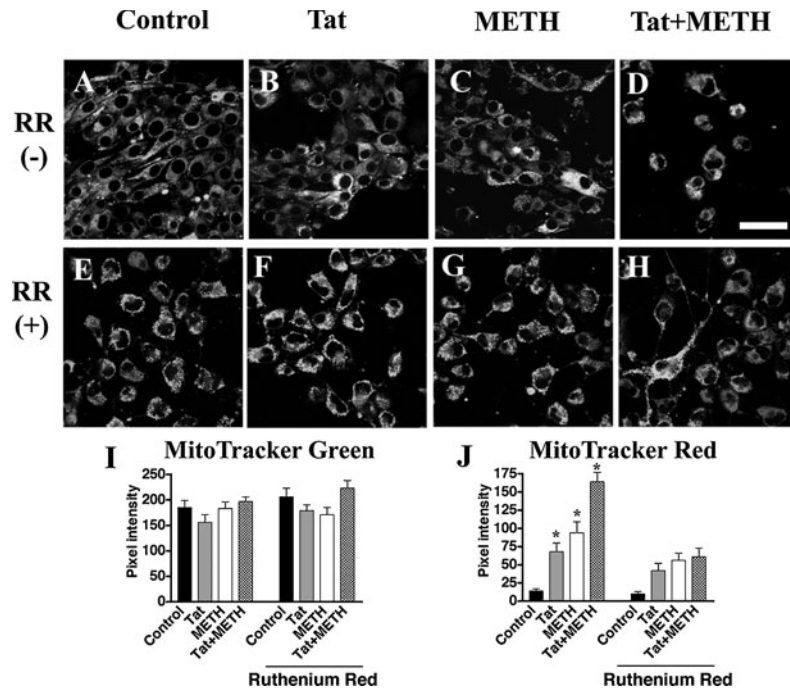
Figure 5 Analyses of mitochondrial alterations in HT22 cells untreated or treated with Tat, METH, or both Tat and METH, and stained with mitochondrial-specific dyes to measure mitochondrial mass and oxidative stress levels. Cells are double stained with MitoTracker Green (*green*) and MitoTracker Red (*red*) and imaged with the laser scanning confocal microscope. Panels **A** to **D** are HT22 cells untreated (**A**), 50 nM Tat (**B**), 50 μM METH (**C**), or 50 nM Tat and 50 μM METH (**D**) for 24 h without pretreatment with RR. Panels **E** to **H** are HT22 cells exposed to RR for 30 min followed by no further treatment (**E**), 50 nM Tat (**F**), 50 μM METH (**G**), or 50 nM Tat and 50 μM METH (**H**) for 24 h. (**I**) Quantitative image analysis of pixel intensity for mitochondrial mass using MitoTracker Green with and without RR pretreatment. (**J**) Quantitative image analysis of pixel intensity for oxidative stress using MitoTracker Red with and without RR pretreatment. $^*P < .05$ by one-factor ANOVA with Fisher's post hoc test when compared to the untreated control, METH, Tat, or Tat and METH. Bar = 25 microns.

44.1% ($P = .0006$), respectively (Figure 7B, C, F, G, J). Pretreatment with RR prior to exposure of HN cells to a combination of Tat and METH decreased oxidative stress by 70.1% ($P < .0001$; Figure 7D, H, J). No significant differences in mitochondrial mass were observed (Figure 7I). Together, these studies suggest that at 6 h, Tat and METH cooperate to disrupt CB expression (Figure 3), thereby altering mitochondrial calcium flux resulting in oxidative stress and at 24 h, neuronal death (Figures 4–7).
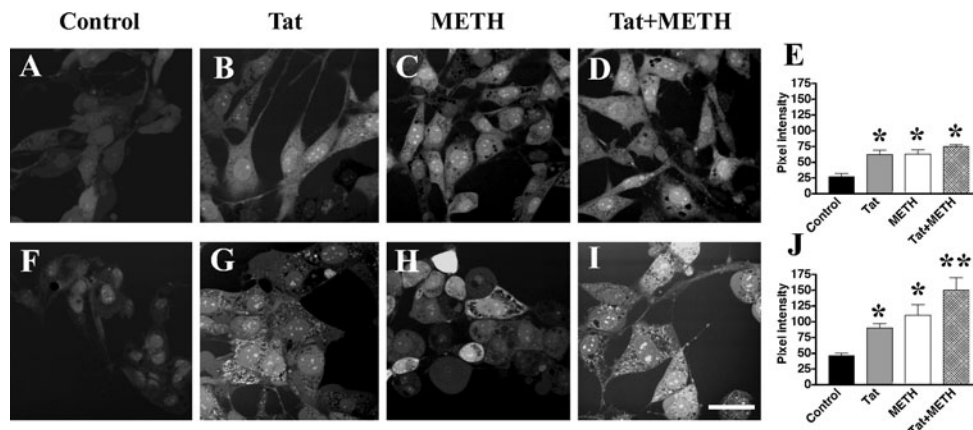

Figure 6 Analyses of oxidative stress in HT22 cells untreated or treated with Tat, METH, or both Tat and METH and stained with H$_2$DCFDA. Panels **A** to **D** and **F** to **I** are LSCM images of representative stained with H$_2$DCFDA. Panels **A** to **D** are HT22 cells untreated (**A**), or treated with Tat (50 nM) (**B**), METH (50 μM) (**C**), or Tat (50 nM) and METH (50 μM) (**D**) for 6 h. Panels **F** to **I** are HT22 cells untreated (**F**), or treated with Tat (50 nM) (**G**), METH (50 μM) (**H**), or Tat (50 nM) and METH (50 μM) (**I**) for 24 h. Panels **E** and **J** show quantitative analyses of levels of fluorescence (pixel intensity) of HT22 cells treated with Tat, METH, or Tat and METH for 6 h (**E**) and 24 h (**J**). Bar = 25 microns.
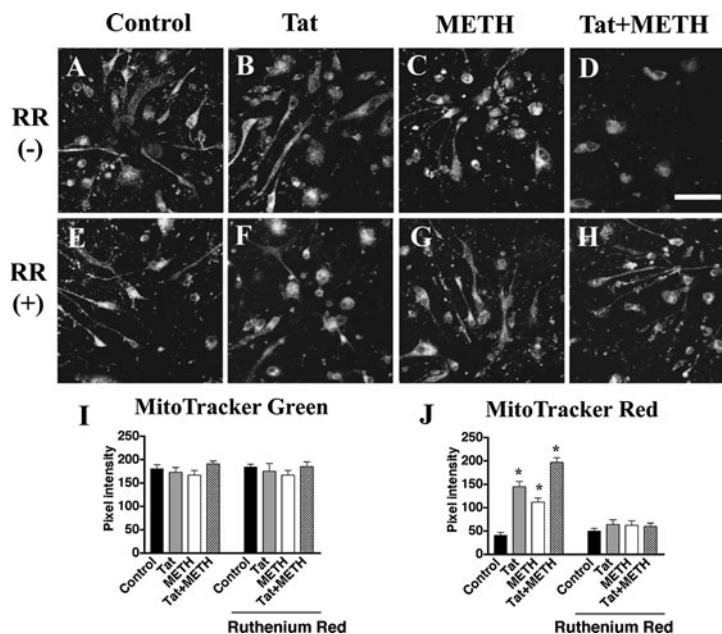
Figure 7 Analyses of mitochondrial alterations in HN cells untreated or treated with Tat, METH, or both Tat and METH and stained with mitochondrial-specific dyes to measure mitochondrial mass and oxidative stress levels. Cells are double stained with MitoTracker Green (*green*) and MitoTracker Red (*red*) and imaged with the laser scanning confocal microscope. Panels **A** to **D** are HN cells untreated (**A**), 250 nM Tat (**B**), 100 μM METH (**C**) or 250 nM Tat and 100 μM METH (**D**) for 24 h without pretreatment with RR. Panels **E** to **H** are HN cells exposed to RR for 30 min followed by no further treatment (**E**), 250 nM Tat (**F**), 100 μM METH (**G**), or 250 nM Tat and 100 μM METH (**H**) for 24 h. (**I**) Quantitative image analysis of pixel intensity for mitochondrial mass using MitoTracker Green with and without RR pretreatment. (**J**) Quantitative image analysis of pixel intensity for oxidative stress using MitoTracker Red with and without RR pretreatment. $^*P < .05$ by one-factor ANOVA with Fisher's post hoc test when compared to the untreated control, METH, Tat, or Tat, and METH. Bar = 25 microns.

Discussion

Supporting previous studies in postmortem brains of HIV-positive METH user patients (Langford *et al*, 2003), the present *in vitro* data indicate that the HIV protein Tat and METH cooperate to promote neuronal damage and cell death in nondopaminergic CB-immunoreactive neurons. Our time course studies suggest that at early stages of exposure, Tat and METH alter cellular CB levels, thereby promoting disruptions in mitochondrial calcium flux that may in turn trigger oxidative stress and cell death after longer exposure. It is possible that in combination, Tat and METH interfere with cell fitness via independent mechanisms or by converging in common pathways leading to cell death. For example, Tat and METH can independently cause cell death by promoting glutamate release, disrupting mitochondria, generating oxygen free radicals or reactive oxygen species, and altering calcium homeostasis (Bonavia *et al*, 2001; Koller *et al*, 2001; New *et al*, 1998). Although excitotoxicity may contribute to the additive effects of Tat and METH *in vivo*, it is unlikely that this mechanism contributed to neurodegeneration in our *in vitro* model because HT22 cells lack the NMDA receptor and the HN cells were only weakly immunoreactive for the NMDA receptor. Thus, other mechanisms involving mitochondrial dysfunction,

oxidative stress, and calcium dysregulation may play a role in neurodegeneration. Supporting a role of these mechanisms in neurodegeneration, the present study showed that pretreatment with the mitochondrial calcium flux blocker RR ameliorated cell death caused by Tat and/or METH. However, blocking calcium flux elsewhere in the cell had no significant effects, suggesting that mitochondrial alterations play a role in the combined neurotoxicity of Tat and METH. However, these results should be interpreted with caution because the calcium flux inhibitors RR and CC may also affect aspects of cell signaling other than calcium modulation (Del Toro *et al*, 2003; Griffiths, 2000; Ying *et al*, 1991). The use of additional methods, including cell labeling with MitoTracker dyes and H_2DCFDA, were used to address mitochondrial function and oxidative stress and to confirm the specificity of our results. Confocal image analyses of cells treated with Tat, METH, or Tat plus METH and labeled with MitoTracker dyes and H_2DCFDA support data from the calcium inhibitor studies.

The relationship between mitochondrial dysfunction and CB expression has not yet been entirely elucidated; however, because CB is responsible, in part, for maintaining calcium homeostasis by binding calcium ions, disruption of its buffering capacity could lead to mitochondrial toxicity by increasing membrane permeability (Rego and Oliveira, 2003).

Tat and methamphetamine in neuronal toxicity
D Langford *et al*
334

Consistent with these findings, the present study shows an increase in MitoTracker Red reactivity in cells treated with Tat and/or METH and these effects were ameliorated by pretreatment with RR. This is consistent with previous studies indicating that Tat and METH interact to cause mitochondrial dysfunction via oxidative stress in neurons (Flora *et al*, 2003; Turchan *et al*, 2001). Thus, in nondopaminergic CB-immunoreactive interneurons, Tat and METH may interfere with the calcium-binding capacity by interfering with the expression of buffering proteins such as CB, leading to changes in mitochondrial function and calcium homeostasis. Tat has been shown to alter calcium homeostasis in neurons and astrocytes, leading to disruption of glutamatergic transmission (Ramirez *et al*, 2001). Likewise, METH not only induces the release of dopamine, noradrenalin, and serotonin, but also binds their receptors (Amano *et al*, 2002), which may lead to intracellular calcium alterations, as described above. Because both Tat and METH independently disrupt calcium currents, it is possible that in combination, these factors converge to further dysregulate calcium homeostasis and mitochondrial function.

In conclusion, this study shows that the combined effects of the HIV protein Tat and METH selectively damage CB-immunoreactive nonpyramidal neurons via mitochondrial dysregulation, suggesting that in combination, these neurotoxins might converge in similar pathways to increase cell injury and death, thereby exacerbating neurobehavioral alterations associated with HIVE and METH use (Taylor *et al*, 2000).

Materials and methods

HT22 culture and treatments
The effects of METH and/or Tat on cell viability were investigated in HT22 cells, a mouse hippocampal cell line derived from the HT4 cell line (Tan *et al*, 1998). The HT22 cell line was chosen because previous studies have shown that this neuronal line, derived from fetal hippocampal cells, is vulnerable to excitotoxic challenge in a manner similar to that reported for HIV proteins (Hashimoto *et al*, 2002). Furthermore, our previous studies in human brains have shown that CB-immunoreactive neurons in the neocortex, basal ganglia, and hippocampus are susceptible to the neurotoxic effects of HIV, therefore, for the *in vitro* studies we screened for a neuronal cell line that would express high levels of CB and display some features of inhibitory neurons, such as the expression of GABA. In preliminary studies comparing the levels of CB expression among several neuronal cell lines, including B103, PC12, and SHSY-5Y cells, it was found that HT22 cells expressed the highest levels of CB immunoreactivity. HT22 cells were maintained at no greater than 70% confluence in 10% fetal bovine serum (FBS) in Dulbecco's Modi-

fied Eagle Medium (DMEM, high glucose; Irvine Scientific, Irvine, CA) with 1 mM L-glutamine, 1 mM sodium pyruvate, and 1% penicillin/streptomycin (GIBCO/BRL, Bethesda, MD). Briefly, cells were routinely grown in DMEM, incubated at 37°C in 5% CO_2 and the medium was replaced every 2 days. Prior to all treatments and experiments, cells were preincubated in serum-free medium for 24 h at 37°C, 5% CO_2. Cells were then treated with varying doses and for varying lengths of time with HIV-Tat (86–amino acid recombinant Tat HxB2; NIH AIDS Research and Reference Program, Rockville, MD, or Trinity Biotech, Carlsbad, CA) and/or METH (deoxyephedrine [±METH], Sigma). For dose-response experiments, HT22 cells were exposed to HIV-Tat for 24 h at: 0, 5, 25, 50, 100, and 250 nM. For time course experiments, HT22 were exposed to 50 nM Tat for 0, 6, 12, 24, and 48 h. Cell viability assays were then conducted to determine optimal dosing and duration, essentially as described previously (Hesselgesser and Horuk, 1999). Likewise, HT22 cells were exposed to the following doses of METH: 5, 25, 50, 100, 250 μM for 24 h and to 50 μM METH for 0, 6, 12, 24, and 48 h and assayed for viability. To study the role of calcium in mitochondrial disruption and cell toxicity, neurons were treated with RR (10 μM; Sigma), TH (5 nM; Sigma), or CC (5 μM; Sigma) for 30 min prior to Tat and/or METH exposures. RR blocks mitochondrial calcium flux, TH blocks endoplasmic reticulum calcium flux, and CC blocks calcium flux from the extracellular environment.

Culture and treatments of human neurons
Neurons (HN) (ScienCell Research Laboratories, Sorrento Valley, CA) isolated from human brain were maintained in basal neuronal medium (ScienCell Research Laboratories) with 1% neuronal growth supplement and 1% penicillin/streptomycin. Prior to treatments, HN cells were preincubated in serum-free neuronal growth medium for 24 h at 37°C, 5% CO_2. Dose-response and time course experiments were conducted on HN cells as described above for HT22 cells, using the same concentrations of Tat and METH for the dose response. However, because HN cells were less susceptible to Tat and METH treatments than HT22 cells, the concentrations used for the HN time course experiments were 250 nM and 100 μM, respectively. To study the role of calcium in mitochondrial disruption and cell toxicity, HN cells were treated with RR (10 μM; Sigma), TH (5 nM; Sigma), or CC (5 μM; Sigma) for 30 min prior to Tat and/or METH exposures, as described for HT22 cells.

Cell viability
For trypan blue exclusion assays, HT22 and HN cells from each experimental condition were rinsed with warm phosphate-buffered saline (PBS), harvested, collected by gentle centrifugation, resuspended in a PBS/trypan blue solution (1:1, vol:vol) and counted,

as previously described (Li *et al*, 1997). Briefly, because trypan blue is not permeable across the cell membrane, cells staining blue indicated disruptions in the cell membrane and were counted as dead. TUNEL staining was carried out on neurons, essentially as described previously (Li *et al*, 1997; Hesselgesser *et al*, 1998). Briefly, cells were grown on 12-mm glass coverslips, treated, rinsed with warm PBS, and fixed with 4% paraformaldehyde for 20 min at room temperature. After rinsing with PBS, cells were permeabilized with 1% H_2O_2 in $1\times$ PBS–Tween-20 for 10 min at room temperature, rinsed twice with PBS, and air dried for 2 min. TUNEL analysis was conducted according to the manufacturer's instructions for staining (Roche Diagnostics, Indianapolis, IN). TUNEL-positive cells were detected with 3,3′-diaminobenzidine (DAB; Sigma) and counted with a computer-aided analysis system (Quantimet 570C; Leica, Bannockburn, IL). Cell death was also assayed by fluorescent staining with FA (Sigma) and PI (Sigma), as previously described (Huang *et al*, 1999). Briefly, the FA working solution was prepared by adding 10 μl of stock FA (50 mg FA in 10 ml of acetone) to 2.5 ml PBS. The FA/PI cocktail was prepared by adding 1 μl of FA working solution to 300 μl of PI (1 mg PI in 50 ml PBS). After rinsing once in warm PBS, 20 μl of the FA/PI cocktail was added to the cells on coverslips and incubated 15 min in the dark. Coverslips were placed cell-side up on SuperFrost slides (Fisher Scientific) with antifading medium (Vector) and immediately imaged with LSCM (MRC1024, Bio-Rad).

Analysis of CB expression in cells

Immunocytochemical assessment of CB and other neuronally associated protein expression was performed in HT22 and HN cells plated on poly-L-lysine–coated coverslips for 24 h in serum-free or 0.5% supplemented medium, respectively, and rinsed with PBS. Neurons were then incubated for 24 h in serum-free medium containing either 50 nM Tat protein or 50 μM METH (Gurwell *et al*, 2001). Coverslips were fixed for 25 min at room temperature in 4% paraformaldehyde and incubated overnight with the monoclonal antibodies against CB (1:1000; Sigma), MAP2 (1:20; Chemicon), PV (1:1000; Sigma), GABA (1:100; Chemicon), NMDA (1:1000; Sigma), or glutamate (1:1000; Chemicon, San Diego, CA). Immunoreactivity was detected with fluorescein isothiocyanate (FITC)-conjugated anti-rabbit secondary antibody (Vector) and imaged with

the LSCM (MRC1024, BioRad), as described previously (Everall *et al*, 2001). GFAP (1:500; Chemicon) was used as a negative control for immunoreactivity.

Analyses of mitochondrial potential

For mitochondrial labeling, neurons were plated onto glass coverslips and treated with Tat and/or METH or left untreated. Prior to treatments, cells were preincubated in serum-free medium for 24 h at 37°C, 5% CO_2. Cells were rinsed with warm $1\times$ PBS and incubated in warm PBS containing 1 μM MitoTracker Green (Molecular Probes, Eugene, Oregon) and 1 μM Redox Red (Molecular Probes) for 30 min at 37°C, 5% CO_2. After staining, coverslips with attached cells were carefully rinsed once in warm $1\times$ PBS, placed cell-side up on SuperFrost slides (Fisher Scientific) with antifading medium (Vector), and immediately imaged with LSCM (MRC1024, BioRad). For each condition, a total of 20 cells were imaged and analyzed. Analyses of levels of fluorescent reactivity in the red and green channels were performed using the NIH Image 1.4.3 software. For each channel, levels of pixel intensity were determined with respect to a standard consisting of cells treated with increasing doses of H_2O_2 (10 μM to 500 μM), as described (Buckman *et al*, 2001).

2′,7′-Dichlorofluorescein (DCF) analysis

To determine if free radical production was associated with Tat and/or METH toxicity, H_2DCFDA loading analysis was performed. Briefly, cells were cultured on poly-L-lysine (Sigma)-coated glass coverslips in 24-well plates to 80% confluency. The cell permeable dye, 2′,7′-dichlorodihydrofluorescein diacetate (H_2DCFDA, 37.5 μmol/L; Molecular Probes, Eugene, OR) was added to the media and cells were incubated at 37°C, 5% CO_2 for 15 min and imaged with the LSCM as previously described (Hsu *et al*, 2000).

Statistical analysis

In vitro experiments were conducted in triplicate on blind-coded samples. After the results were obtained, the code was broken and data were analyzed with the StatView program (SAS Institute, North Carolina). Results were analyzed by one-way analysis of variance (ANOVA) with post hoc Dunnett's. Data from the viability assays were analyzed by unpaired two tailed Student's *t* test ($P \leq .05$) with the StatView program (SAS Institute). All results were expressed as mean ± SEM.

References

Aksenov MY, Hasselrot U, Bansal AK, Wu G, Nath A, Anderson C, Mactutus CF, Booze RM (2001). Oxidative damage induced by the injection of HIV-1 Tat protein in the rat striatum. *Neurosci Lett* **305:** 5–8.

Amano T, Matsubayashi H, Sasa M (2002). Alteration of neuronal activities following repeated administration of stimulants. *Nihon Arukoru Yakubutsu Igakkai Zasshi* **37:** 31–40.

Bell JE, Brettle RP, Chiswick A, Simmonds P (1998). HIV encephalitis, proviral load and dementia in drug users and homosexuals with AIDS. Effect of neocortical involvement. *Brain* **121(Pt 11):** 2043–2052.

Berman SB, Hastings TG (1999). Dopamine oxidation alters mitochondrial respiration and induces permeability transition in brain mitochondria: implications for Parkinson's disease. *J Neurochem* **73:** 1127–1137.

Bonavia R, Bajetto A, Barbero S, Albini A, Noonan DM, Schettini G (2001). HIV-1 Tat causes apoptotic death and calcium homeostasis alterations in rat neurons. *Biochem Biophys Res Commun* **288:** 301–308.

Bouwman FH, Skolasky RL, Hes D, Selnes OA, Glass JD, Nance-Sproson TE, Royal W, Dal Pan GJ, McArthur JC (1998). Variable progression of HIV-associated dementia. *Neurology* **50:** 1814–1820.

Buckman JF, Hernandez H, Kress GJ, Votyakova TV, Pal S, Reynolds IJ (2001). MitoTracker labeling in primary neuronal and astrocytic cultures: influence of mitochondrial membrane potential and oxidants. *J Neurosci Methods* **104:** 165-176.

Cadet JL, Brannock C (1998). Free radicals and the pathobiology of brain dopamine systems. *Neurochem Int* **32:** 117–131.

Chesney MA, Barrett DC, Stall R (1998). Histories of substance use and risk behavior: precursors to HIV seroconversion in homosexual men. *Am J Public Health* **88:** 113–116.

Del Toro R, Levitsky KL, Lopez-Barneo J, Chiara MD (2003). Induction of T-type calcium channel gene expression by chronic hypoxia. *J Biol Chem* **278:** 22316–22324.

Eisch A, O'Dell S, Marshall J (1996). Striatal and cortical NMDA receptors are altered by a neurotoxic regimen of methamphetamine. *Synapse* **22:** 217–225.

Everall IP, Trillo-Pazos G, Bell C, Mallory M, Sanders V, Masliah E (2001). Amelioration of neurotoxic effects of HIV envelope protein gp120 by fibroblast growth factor: a strategy for neuroprotection. *J Neuropathol Exp Neurol* **60:** 293–301.

Flora G, Lee YW, Nath A, Hennig B, Maragos W, Toborek M (2003). Methamphetamine potentiates HIV-1 Tat protein-mediated activation of redox-sensitive pathways in discrete regions of the brain. *Exp Neurol* **179:** 60–70.

Griffiths EJ (2000). Use of ruthenium red as an inhibitor of mitochondrial Ca(2+) uptake in single rat cardiomyocytes. *FEBS Lett* **486:** 257–260.

Gurwell JA, Nath A, Sun Q, Zhang J, Martin KM, Chen Y, Hauser KF (2001). Synergistic neurotoxicity of opioids and human immunodeficiency virus-1 Tat protein in striatal neurons in vitro. *Neuroscience* **102:** 555–563.

Hashimoto M, Sagara Y, Everall IP, Mallory M, Everson A, Langford D, Masliah E (2002). Fibroblast growth factor 1 regulates signaling via the GSK3{beta} pathway: implications for neuroprotection. *J Biol Chem* **277:** 32985–32991.

Hesselgesser J, Horuk R (1999). Chemokine and chemokine receptor expression in the central nervous system. *J NeuroVirol* **5:** 13–26.

Hesselgesser J, Taub D, Baskar P, Greenberg M, Hoxie J, Kolson DL, Horuk R (1998). Neuronal apoptosis induced by HIV-1 gp120 and the chemokine SDF-1alpha is mediated by the chemokine receptor CXCR4. *CurrBiol* **8:** 595–598.

Hsu LJ, Sagara Y, Arroyo A, Rockenstein E, Sisk A, Mallory M, Wong J, Takenouchi T, Hashimoto M, Masliah E (2000). *α*-Synuclein promotes mitochondrial deficiencies and oxidative stress. *Am J Pathol* **157:** 401–410.

Huang M-B, Hunter M, Bond V (1999). Effect of extracellular human immunodeficiency virus Type 1 glycoprotein 120 on primary human vascular edothelial cell cultures. *AIDS Res Human Retroviruses* **15:** 1265–1277.

Imam SZ, Ali SF (2000). Selenium, an antioxidant, attenuates methamphetamine-induced dopaminergic toxicity and peroxynitrite generation. *Brain Res* **855:** 186–191.

Koller H, Schaal H, Freund M, Garrido SR, von Giesen HJ, Ott M, Rosenbaum C, Arendt G (2001). HIV-1 protein Tat reduces the glutamate-induced intracellular Ca^{2+} increase in cultured cortical astrocytes. *Eur J Neurosci* **14:** 1793–1799.

Kruman II, Nath A, Mattson MP (1998). HIV-1 protein Tat induces apoptosis of hippocampal neurons by a mechanism involving caspase activation, calcium overload, and oxidative stress. *Exp Neurol* **154:** 276–288.

Langford D, Adame A, Grigorian A, Grant I, McCutchan JA, Ellis RJ, Marcotte TD, Masliah E, the HIV Neurobehavioral Research Center (2003). Patterns of selective neuronal damage in methamphetamine-user AIDS patients. *J Acquir Immune Defic Syndr* **34:** 467–474.

Li HL, Roch J-M, Sundsmo M, Otero D, Sisodia S, Thomas R, Saitoh T (1997). Defective neurite extension is caused by a mutation in amyloid ß/A4 (Aß) protein precursor found in familial Alzheimer's disease. *J Neurobiol* **32:** 469–480.

Love S (1999). Oxidative stress in brain ischemia. *Brain Pathol* **9:** 119–131.

Molitor F, Ruiz JD, Flynn N, Mikanda JN, Sun RK, Anderson R (1999). Methamphetamine use and sexual and injection risk behaviors among out-of-treatment injection drug users. *Am J Drug Alcohol Abuse* **25:** 475–493.

Nath A, Hauser KF, Wojna V, Booze RM, Maragos W, Prendergast M, Cass W, Turchan JT (2002). Molecular basis for interactions of HIV and drugs of abuse. *J Acquir Immune Defic Syndr* **31(Suppl 2):** S62–S69.

Nath A, Maragos WF, Avison MJ, Schmitt FA, Berger JR (2001). Acceleration of HIV dementia with methamphetamine and cocaine. *J NeuroVirol* **7:** 66–71.

New DR, Maggirwar SB, Epstein LG, Dewhurst S, Gelbard HA (1998). HIV-1 Tat induces neuronal death via tumor necrosis factor-alpha and activation of non-*N*-methyl-D-aspartate receptors by a NFkappaB-independent mechanism. *J Biol Chem* **273:** 17852–17858.

Ohmori T, Abekawa T, Koyama T (1996). The role of glutamate in behavioral and neurotoxic effects of methamphetamine. *Neurochem Int* **29:** 301–307.

Poot M, Zhang YZ, Kramer JA, Wells KS, Jones LJ, Hanzel DK, Lugade AG, Singer VL, Haugland RP (1996). Analysis of mitochondrial morphology and function with novel fixable fluorescent stains. *J Histochem Cytochem* **44:** 1363-1372.

Ramirez SH, Sanchez JF, Dimitri CA, Gelbard HA, Dewhurst S, Maggirwar SB (2001). Neurotrophins prevent HIV Tat-induced neuronal apoptosis via a nuclear factor-kappaB (NF-kappaB)-dependent mechanism. *J Neurochem* **78:** 874–889.

Rego AC, Oliveira CR (2003). Mitochondrial dysfunction and reactive oxygen species in excitotoxicity and apoptosis: implications for the pathogenesis of neurodegenerative diseases. *Neurochem Res* **28:** 1563–1574.

Stephans S, Yamamoto B (1994). Methamphetamine-induced neurotoxicity: roles for glutamate and dopamine efflux. *Synapse* **17:** 203–209.

Stout AK, Raphael HM, Kanterewicz BI, Klann E, Reynolds IJ (1998). Glutamate-induced neuron death requires mitochondrial calcium uptake. *Nat Neurosci* **1:** 366–373.

Tan S, Sagara Y, Liu Y, Maher P, Schubert D (1998). The regulation of reactive oxygen species production during programmed cell death. *J Cell Biol* **141:** 1423–1432.

Taylor MJ, Alhassoon OM, Schweinsburg BC, Videen JS, Grant I (2000). MR spectroscopy in HIV and stimulant dependence HNRC Group. HIV Neurobehavioral Research Center. *J Int Neuropsychol Soc* **6:** 83–85.

Turchan J, Anderson C, Hauser KF, Sun Q, Zhang J, Liu Y, Wise PM, Kruman I, Maragos W, Mattson MP, Booze R, Nath A (2001). Estrogen protects against the synergistic toxicity by HIV proteins, methamphetamine and cocaine. *BMC Neurosci* **2:** 3.

Ying WL, Emerson J, Clarke MJ, Sanadi DR (1991). Inhibition of mitochondrial calcium ion transport by an oxo-bridged dinuclear ruthenium ammine complex. *Biochemistry* **30:** 4949–4952.